A research on GRP-based high resolution and efficient ghost fluid method

Speaker: Zhixin Huo

Advisors: Jiequan Li, Zupeng Jia

Beijing Institute of Applied Physics and Computational Mathematics

Graduate School of China Academy of Engineering Physics

May 1, 2023

Catalogue

1. Research background

➢The practical application of compressible multi-medium problems

Underwater explosion

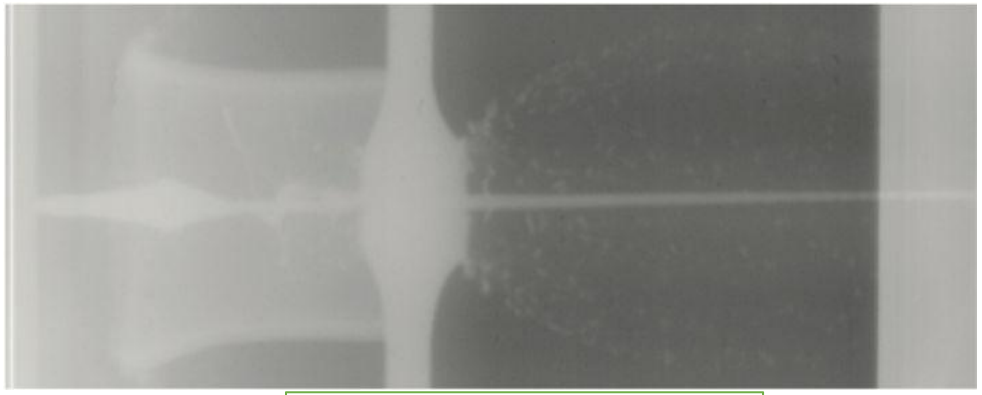

Jet armour piercing

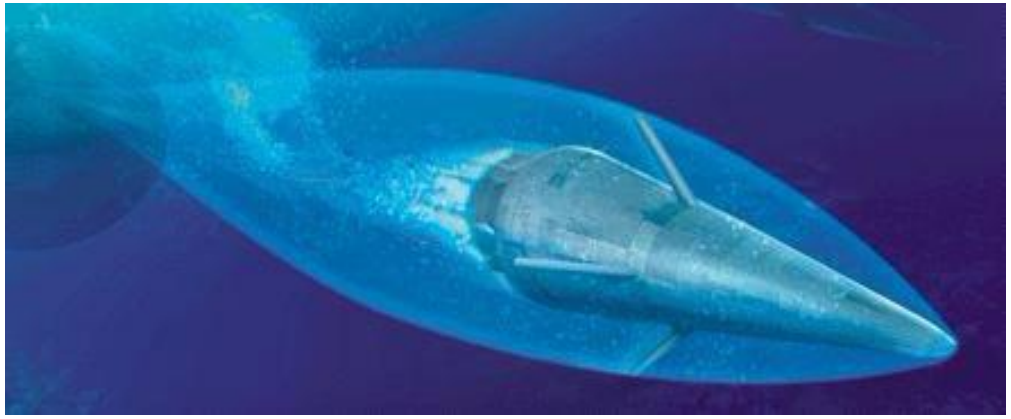

Supercavitating torpedo

Propeller cavitation

Figure 1.1 The practical application of compressible multi-medium problems.

★ Immiscible interface：
level set， front tracking and so on

★ Two different mediums：
different EOS

★ Control equations：
Euler equations

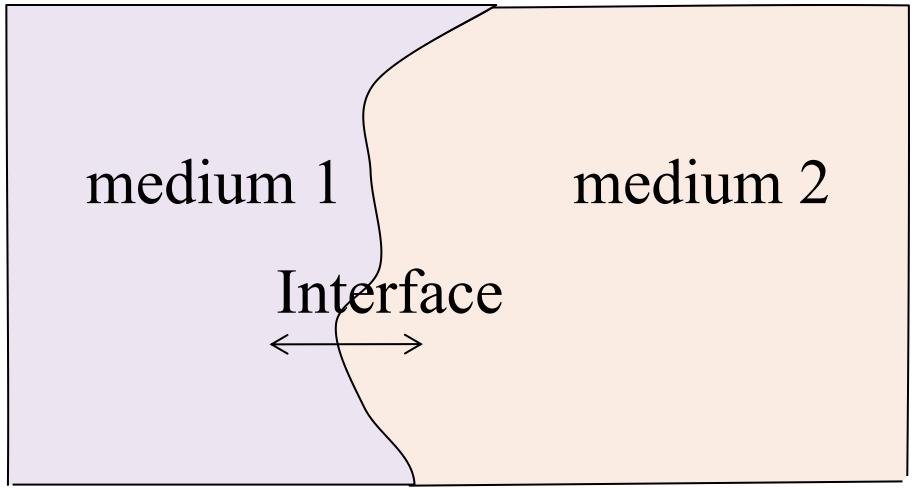

Figure 1.2 the model for multi-medium fluid flows

2. Ghost fluid method（GFM）

➢ The main idea of GFM

By defining ghost fluid regions and ghost fluid states, a multi-medium problem can be decoupled into several single-medium problems, which can be solved seperately.

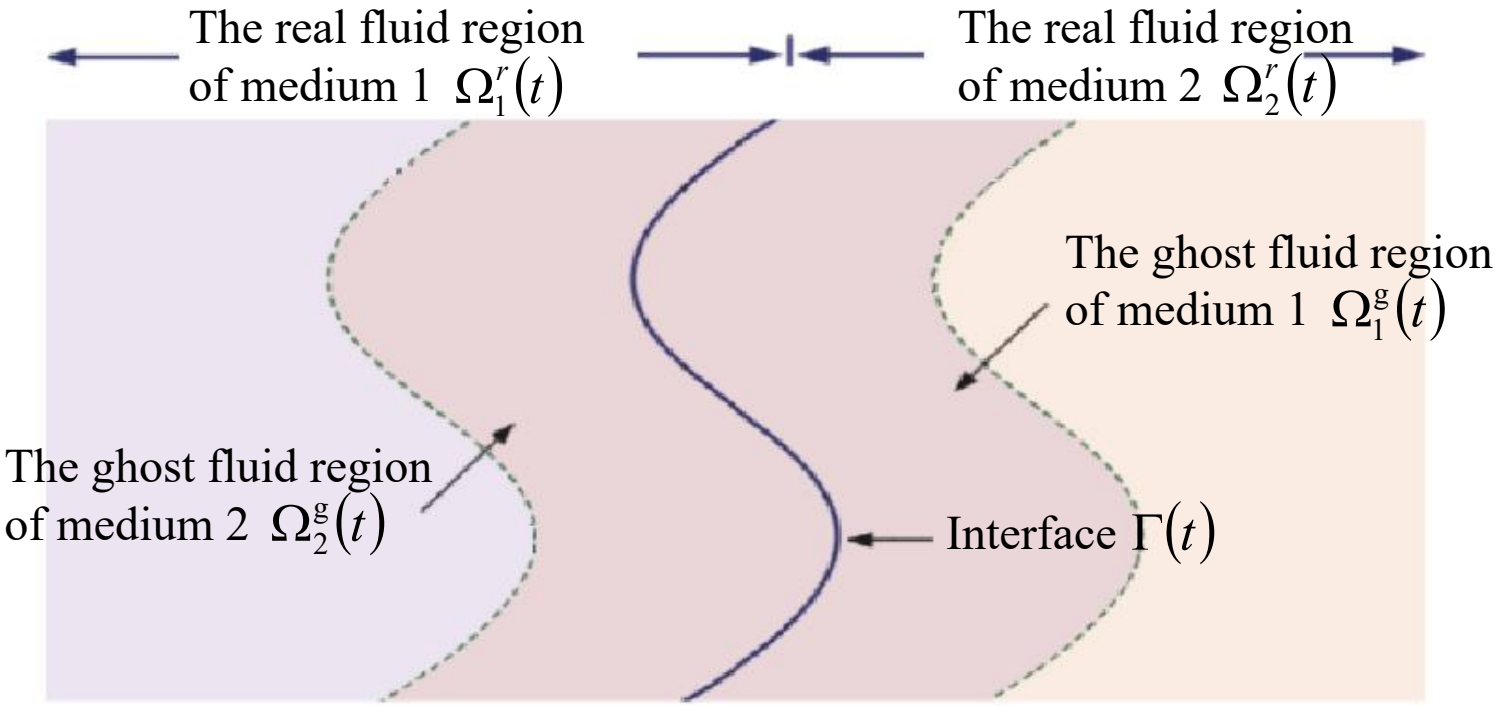

Figure 2.1 The main idea of GFM.

➢ The origin and development of GFM

Different GFM differ in the way how the ghost fluid states are defined.

★ Define ghost fluid states by extrapolation from the real fluid regions

- （**OGFM**）Fedkiw R P , Aslam T , Merriman B , et al. A Non-oscillatory Eulerian Approach to Interfaces in Multimaterial Flows (the Ghost Fluid Method)[J]. Journal of Computational Physics, 1999, 152(2):457-492.
- （**GWGFM**）Fedkiw R P . Coupling an Eulerian Fluid Calculation to a Lagrangian Solid Calculation with the Ghost Fluid Method[J]. Journal of Computational Physics, 2002, 175(1):200-224.
- .....

★ Define ghost fluid states by a local double-medium Riemann problem

- （**MGFM**）

（1）Liu T G, Khoo B C, Yeo K S . Ghost fluid method for strong shock impacting on material interface[J]. Journal of Computational Physics, 2003.

（2）Liu T G , Khoo B C , Wang C W . The ghost fluid method for compressible gas-water simulation[J]. Journal of Computational Physics, 2005, 204(1):193-221.

- （**RGFM**）Wang C W , Liu T G , Khoo B C . A Real Ghost Fluid Method for the Simulation of Multimedium Compressible Flow[J]. Siam Journal on Scientific Computing, 2006, 28(1):278-302.
- （**PGFM**）Xu L, Feng CL, Liu T G. Practical techniques in ghost fluid method for compressible multi-medium flows [J]. Commun. Comput. Phys., 2016, 20:619-659.
- （**IGFM**）Hu X Y , Khoo B C . An interface interaction method for compressible multifluids[J]. Journal of Computational Physics, 2004, 198(1):35-64.
- .....

3. One-dimensional compressible multi-medium problem

➢ Mathematical model

The source term

$$\frac{\partial U}{\partial t}+\frac{\partial F(U)}{\partial x}=\boxed{H(x,U),}\ \text{for}\ x\in(a,b),\ t>0,$$

$$U(x,0)=\begin{cases}U_1(x,0), & \text{if } x\in(a,x_\Gamma^0),\\ U_2(x,0), & \text{if } x\in(x_\Gamma^0,b),\end{cases}\qquad (3.1)$$

$$e=\begin{cases}e_1(\rho,p), & \text{if } x\in(a,x_\Gamma(t)),\\ e_2(\rho,p), & \text{if } x\in(x_\Gamma(t),b).\end{cases}$$

Let the interface be $\Gamma(t): x=x_\Gamma(t)$.

Denote $\Gamma^n=\Gamma(t_n),\ n=0,1,2,\cdots,$

The EOS of medium J is $e=e_J(\rho,p),\ J=1,2.$

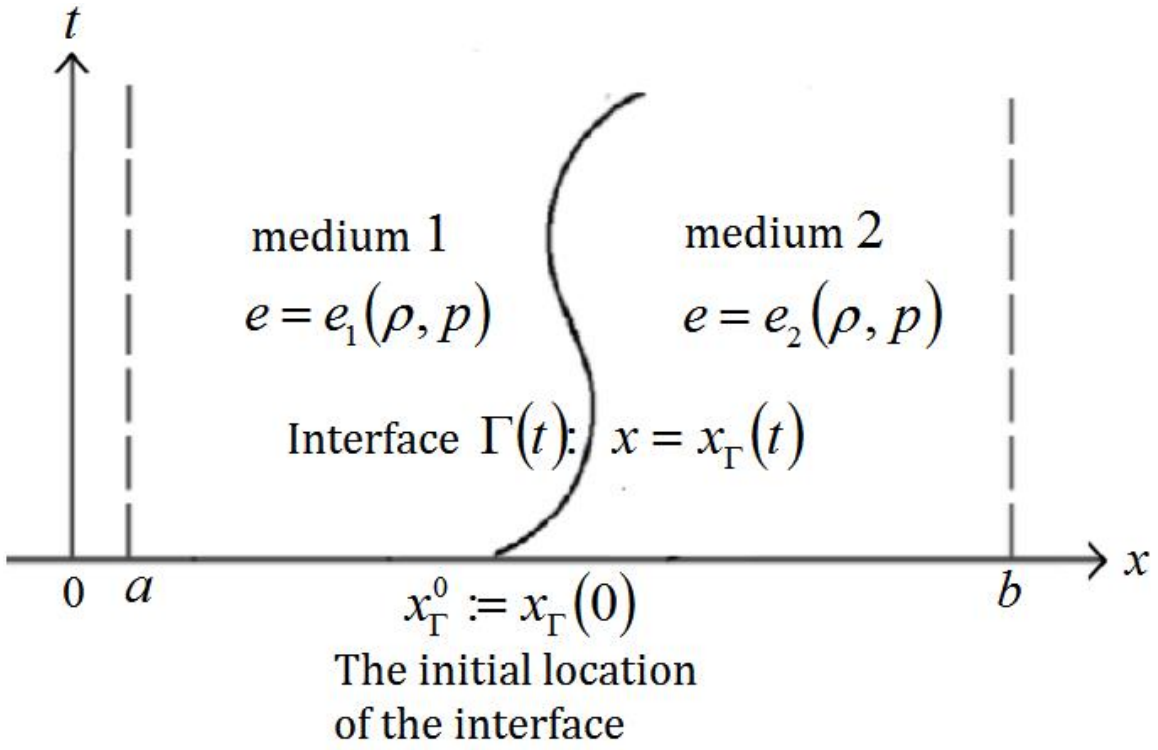

Figure 3.1 The mathematical model for one-dimensional compressible multi-medium problem.

➢ Riemann problem（RP）-based GFM in 1D

A local double - medium RP is established at the interface:

The source term is zero

$$\frac{\partial U}{\partial t}+\frac{\partial F(U)}{\partial x}=0,\quad \text{for } t>t_n, x\in\left(x_\Gamma^n-\delta, x_\Gamma^n+\delta\right),$$

$$U(x,t_n)=\begin{cases}U_1, & \text{if } x<x_\Gamma^n,\\ U_2, & \text{if } x>x_\Gamma^n,\end{cases}\qquad e=\begin{cases}e_1(\rho,p), & \text{if } x<x_\Gamma(t),\\ e_2(\rho,p), & \text{if } x>x_\Gamma(t).\end{cases}\tag{3.2}$$

where the associated vector of primitive variables for the vector of conserved variable U_J is $W_J, J=1,2.$

Assuming that the interface $x_\Gamma^n\in[x_i,x_{i+1}]$, then chose $W_1:=W_{i-1}^n,\quad W_2:=W_{i+2}^n.$

The initial data are linearly distributed

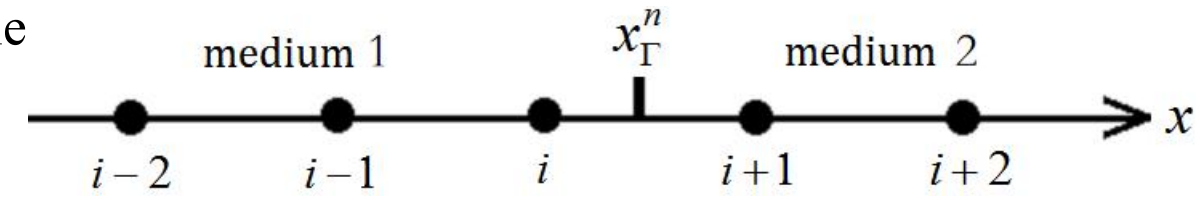

Figure 3.2 The choice for the initial data of the local double-medium problem (3.2).

The intermediate states are also constantly distributed

As shown in Picture 3.3, solve the intermediate states of the local double - medium problem (3.2),

$$W_{J*} = (\rho_{J*}, u_*, p_*)^T, \quad J = 1,2.$$

Define the fluid states in the ghost fluid regions and the real fluid regions near the interface of medium J as U_{J*}, where U_{J*} is the vector of conserved variables for the vector of primitive variables W_{J*}.

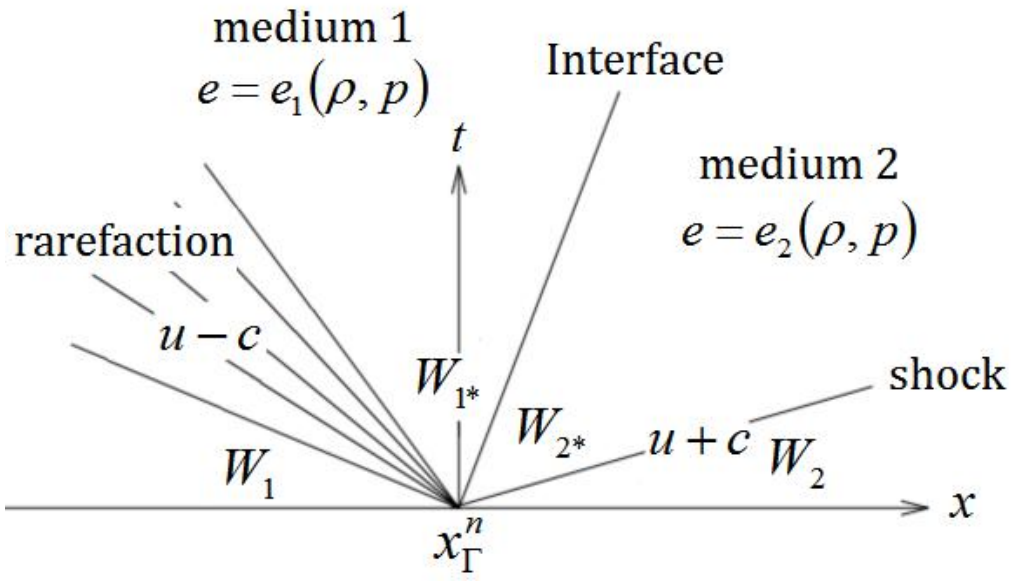

Figure 3.3 The wave structure of local double -medium GRP (3.2) .

✓ The disadvantages of the RP-based GFM in 1D

There will be pressure mismatch errors near the interface, and this kind of errors will accumulated over time.

Assuming that $p\left(x_\Gamma^n-0,t_n\right)=p\left(x_\Gamma^n+0,t_n\right)$, consider the pressure mismatch errors at the interface during the time step $\left[t_n,t_{n+1}\right]$. By Taylor expansion respect to time t, we have

$$p\left(x_\Gamma^{n+1}\pm 0,t_{n+1}\right)=p\left(x_\Gamma^n\pm 0,t_n\right)+\Delta t\frac{Dp}{Dt}\left(x_\Gamma^n\pm 0,t_n\right)+O\left(\Delta t^2\right),\quad \text{where } \frac{Dp}{Dt}=\frac{\partial p}{\partial t}+u_\Gamma\frac{\partial p}{\partial x},\quad u_\Gamma=x_\Gamma'(t).$$

Then we have $E^n(p)=p\left(x_\Gamma^{n+1}+0,t_{n+1}\right)-p\left(x_\Gamma^{n+1}-0,t_{n+1}\right)=\left[\frac{Dp}{Dt}\left(x_\Gamma^n+0,t_n\right)-\frac{Dp}{Dt}\left(x_\Gamma^n-0,t_n\right)\right]\Delta t+O\left(\Delta t^2\right).$

For the ghost fluid states defined by the RP - based GFM, in general we have $\frac{Dp}{Dt}\left(x_\Gamma^n+0,t_n\right)\neq\frac{Dp}{Dt}\left(x_\Gamma^n-0,t_n\right).$

Especially for radially symmetric flows, we have $\frac{Dp}{Dt}+\rho c^2\frac{\partial u}{\partial x}=-\frac{m-1}{x}\rho c^2u$. As $\frac{\partial u}{\partial x}\left(x_\Gamma^n+0,t_n\right)=\frac{\partial u}{\partial x}\left(x_\Gamma^n-0,t_n\right)=0,$

then $\frac{Dp}{Dt}\left(x_\Gamma^n+0,t_n\right)-\frac{Dp}{Dt}\left(x_\Gamma^n-0,t_n\right)=-\frac{m-1}{x_\Gamma^n}u_*\left[\gamma_2\left(p_*+p_\infty^2\right)-\gamma_1\left(p_*+p_\infty^1\right)\right]\neq 0$, i.e.

$$E_{\mathrm{RP}}^n(p)=O(\Delta t),\quad E_{\mathrm{RP}}(P)=\sum_n E_{\mathrm{RP}}^n(p)=O(1).$$

The cause of the pressure mismatch errors: the spatial derivatives of the ghost fluid states defined by the RP based GFM are zero, which can not reflect the effects of the source terms in the equations. Therefore they can not maintain the continuity of the material derivatives of pressure.

➢ Generalized Riemann problem（GRP）-based GFM in 1D

Establish a local double-medium GRP at the interface:

$$\frac{\partial U}{\partial t}+\frac{\partial F(U)}{\partial x}=H(x,U), \quad \text{for } t>t_n, x\in\left(x_\Gamma^n-\delta, x_\Gamma^n+\delta\right), \tag{3.3}$$

The source term of (3.1)

$$U(x,t_n)=\begin{cases}U_1(x), & \text{if } x<x_\Gamma^n,\\ U_2(x), & \text{if } x>x_\Gamma^n,\end{cases} \qquad e=\begin{cases}e_1(\rho,p), & \text{if } x<x_\Gamma(t),\\ e_2(\rho,p), & \text{if } x>x_\Gamma(t).\end{cases}$$

where $U_{\mathrm{J}}(x)$ is the vector of conserved variables for the the vector of primitive variables $W_{\mathrm{J}}+(x-\bar{x}_{\mathrm{J}})W_{\mathrm{J}}'$, $\mathrm{J}=1,2$. Assuming that the interface $x_\Gamma^n\in[x_i,x_{i+1}]$, then chose

$$\bar{x}_1=x_{i-1}, \bar{x}_2=x_{i+2},$$

and

$$W_1=W_{i-1}^n,\ W_1'=\left(\frac{\partial W}{\partial x}\right)_{i-1}^n, \quad W_2=W_{i+2}^n, W_2'=\left(\frac{\partial W}{\partial x}\right)_{i+2}^n.$$

The primitive variables in the initial data are linearly distributed

As shown in Figure 3.4, firstly, choose the following (3.4) as the initial data of the associated RP of the local double - medium GRP (3.3),

$$U(x,t_n)=\begin{cases}\widetilde{U}_1, & \text{if } x<x_\Gamma^n,\\ \widetilde{U}_2, & \text{if } x>x_\Gamma^n,\end{cases} \tag{3.4}$$

where the vector of primitive variables associated with the vector of conserved variables $\widetilde{U}_J$ is $W_J+\left(x_\Gamma^n-x_J\right)W_J'$, $J=1,2$, to obtain the intermediate states

$$\widetilde{W}_{J*}=\left(\widetilde{\rho}_{J*},\widetilde{u}_*,\widetilde{p}_*\right)^T,\quad J=1,2. \tag{3.5}$$

Then choose W_J', $J=1,2$, as the initial data of the double - medium GRP (3.3) to obtain the spatial derivatives of the intermediate states

$$W_{J*}'=\left(\left(\frac{\partial\rho}{\partial x}\right)_{J*},\left(\frac{\partial u}{\partial x}\right)_{J*},\left(\frac{\partial p}{\partial x}\right)_{J*}\right)^T,\quad J=1,2. \tag{3.6}$$

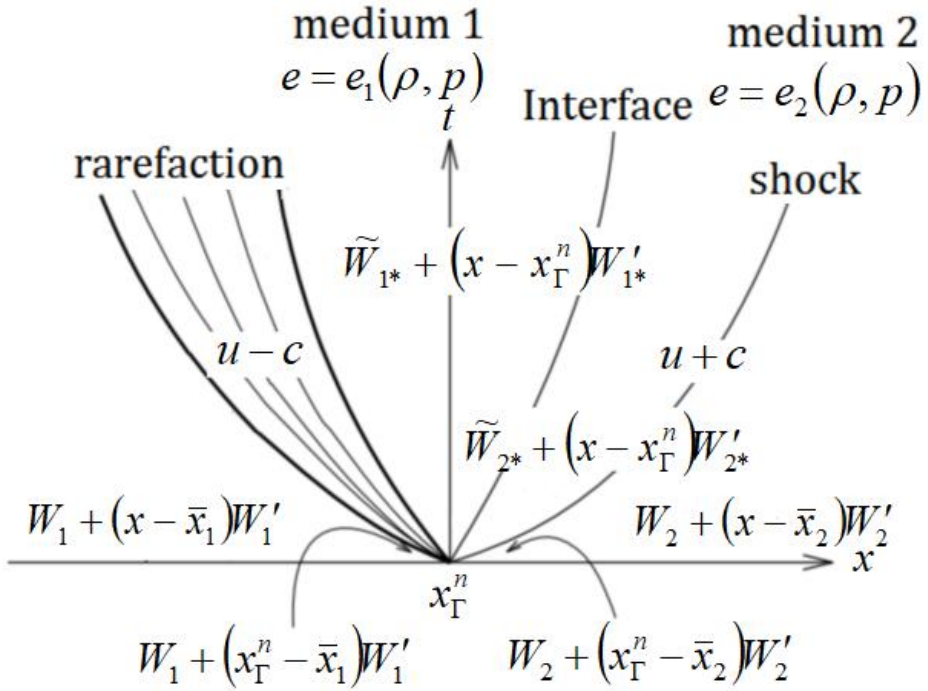

Figure 3.4 The wave structure of local double -medium GRP (3.3) .

The primitive variables in the intermediate states are linearly distributed in computation

Define the fluid states in the ghost fluid region and the real fluid region near the interface of medium J as $\widetilde{W}_{J*}+\left(x-x_\Gamma^n\right)W_{J*}'$, $J=1,2$. The spatial derivatives of the fluid states in these nodes are defined as W_{J*}', $J=1,2$.

The spatial derivatives of the intermediate states （3.6）of the double-medium GRP（3.3）:

We establish the equation for the material derivatives of pressure and velocity for each medium, and then according to the continuity of the material derivatives of pressure and velocity across the interface, i.e.,

$$\left(\frac{Du}{Dt}\right)_{1*}=\left(\frac{Du}{Dt}\right)_{2*}\overset{\Delta}{=}\left(\frac{Du}{Dt}\right)_{*},\quad \left(\frac{Dp}{Dt}\right)_{1*}=\left(\frac{Dp}{Dt}\right)_{2*}\overset{\Delta}{=}\left(\frac{Dp}{Dt}\right)_{*},\quad \text{where } D/Dt=\partial/\partial t+u\partial/\partial x,$$

combine them together to obtain

$$\begin{cases} a_1\left(\frac{Du}{Dt}\right)_{*}+b_1\left(\frac{Dp}{Dt}\right)_{*}=d_1, \\ a_2\left(\frac{Du}{Dt}\right)_{*}+b_2\left(\frac{Dp}{Dt}\right)_{*}=d_2, \end{cases}$$

where the effects of the source $H(x,U)$ are contained in the coefficients d_1 and d_2. Then we can obtain the spatial derivatives of pressure and velocity by combining the 1D Euler equations.

The spatial derivatives of density for each medium are obtained respectively.

✓ The advatages of the GRP-based GFM in 1D

- Eliminate the pressure mismatch errors , even for long time simulation.

The ghost fluid states defined by the GRP - based GFM can guarantee that

$$\frac{Dp}{Dt}\left(x_\Gamma^n - 0, t_n\right) = \frac{Dp}{Dt}\left(x_\Gamma^n + 0, t_n\right).$$

Then during the time step $[t_n, t_{n+1}]$, the pressure mismatch errors at the interface are

$$\begin{aligned} E_{\mathrm{GRP}}^n(p) &= p\left(x_\Gamma^{n+1} + 0, t_{n+1}\right) - p\left(x_\Gamma^{n+1} - 0, t_{n+1}\right) \\ &= \left[\frac{Dp}{Dt}\left(x_\Gamma^n + 0, t_n\right) - \frac{Dp}{Dt}\left(x_\Gamma^n - 0, t_n\right)\right]\Delta t + O\left(\Delta t^2\right) \\ &= O\left(\Delta t^2\right), \end{aligned}$$

during the whole computation time $[0, T]$, the pressure mismatch errors at the interface are

$$E_{\mathrm{GRP}} = \sum_n E_{\mathrm{GRP}}^n(p) = O(\Delta t).$$

Improve the computation accuracy

Reason 1:

The initial data of the associated RP of the local double - medium (3.3) is

$$U(x,t_n)=\begin{cases}\widetilde{U}_1, & \text{if } x<x_\Gamma^n,\\ \widetilde{U}_2, & \text{if } x>x_\Gamma^n,\end{cases}$$

where the vector of primitive variables associated with the vector of conserved variables $\widetilde{U}_J$ is $W_J+(x_\Gamma^n-x_J)W_J'$, $J=1,2$, the computation accuracy is second order.

The initial data of the local double - medium RP (3.2) is

$$U(x,t_n)=\begin{cases}U_1, & \text{if } x<x_\Gamma^n,\\ U_2, & \text{if } x>x_\Gamma^n,\end{cases}$$

where the vector of primitive variables associated with the vector of conserved variables U_J is W_J, $J=1,2$, the computation accuracy is first order.

Reason 2:

The ghost fluid states defined by the GRP - based GFM are linearly distributed, the spatial derivatives of which are not zero; while the ghost fluid states defined by the RP - based GFM are constantly distributed, the spatial derivatives of which are zero.

✓ Numerical results in 1D

Example: Underwater explosion of radial symmetric flow.

The source term of the radial symmetric flow is

$$H(x,U)=-\frac{m-1}{x}\left(\rho u,\rho u^2,u(\rho E+p)\right)^T,\quad x>0,$$

where x is the radial coordinate, $m=2$ for cylindrical symmetrical flows, and $m=3$ for spherical symmetrical flows.

The underwater radial symmetrical explosion is as shown in Figure 3.5, where gas is inside, and water is outside.

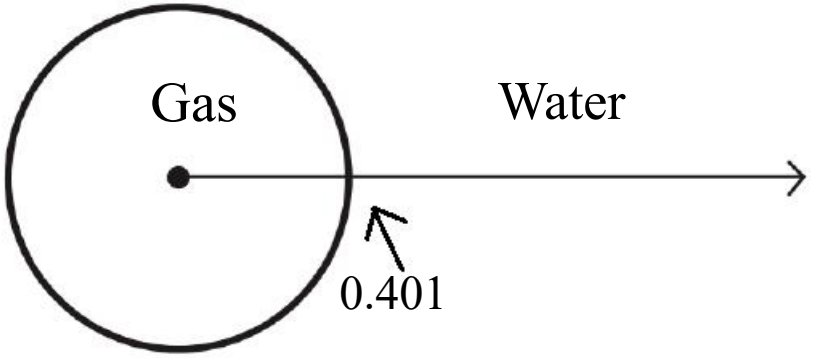

Figure 3.5 Underwater explosion of radial symmetric flow.

The EOS of both mediums are represented as $e=\dfrac{p+\gamma_J p_{\infty,J}}{(1-\gamma_J)\rho}$.

The initial data are

$$\begin{cases}(\rho_1,u_1,p_1,\gamma_1,p_{\infty,1})=(1.27,0.0,8290.91,1.4,0.0), & x\in(0,0.401),\\ (\rho_2,u_2,p_2,\gamma_2,p_{\infty,2})=(1.0,0.0,1.0,7.0,3000.0), & x\in(0.401,12.0).\end{cases}$$

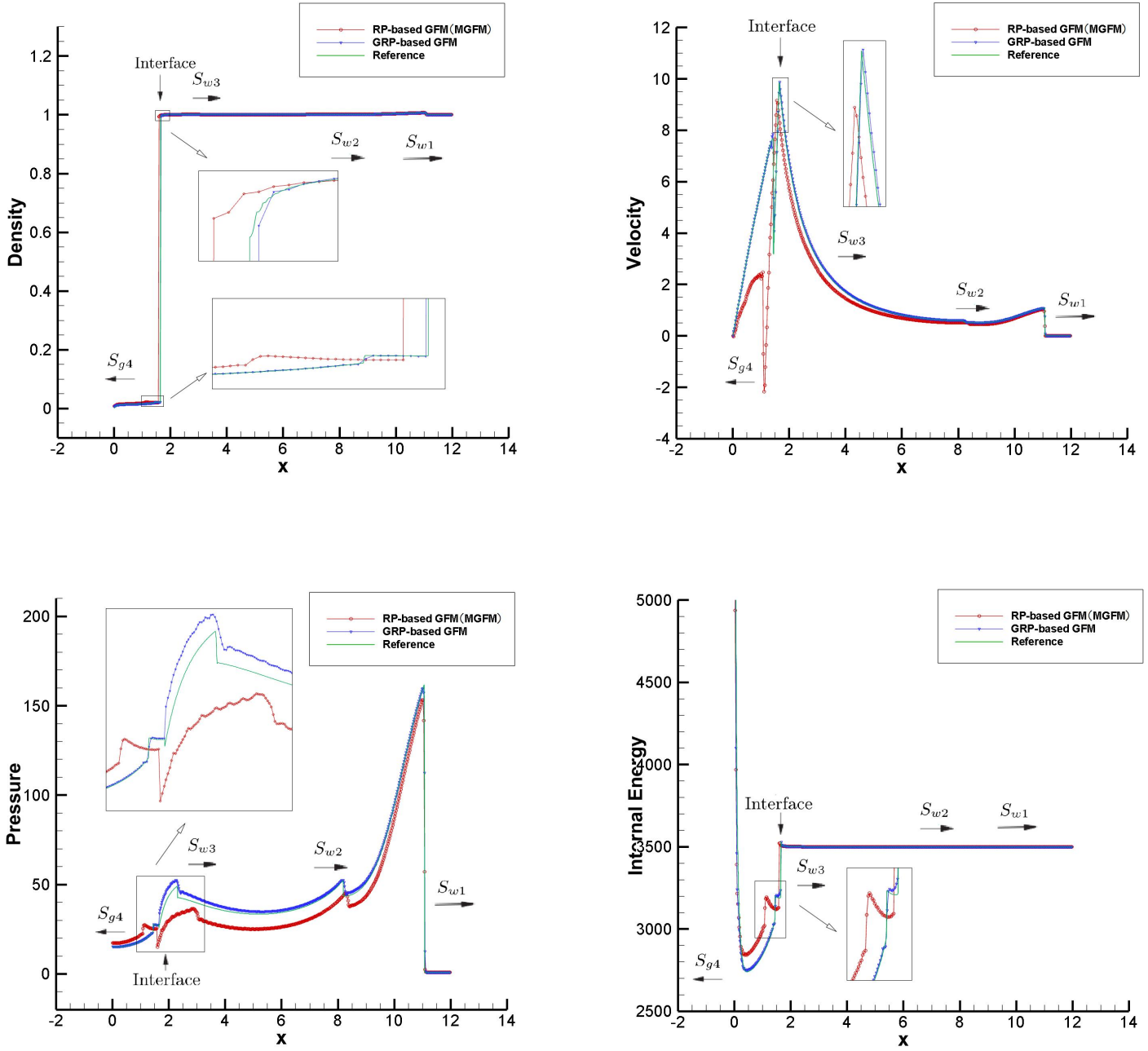

Figure 3.6 Underwater spherical symmetrical explositon $(m = 3)$.

The fineness of the mesh is 1/500, the computation time is $t = 0.07$.

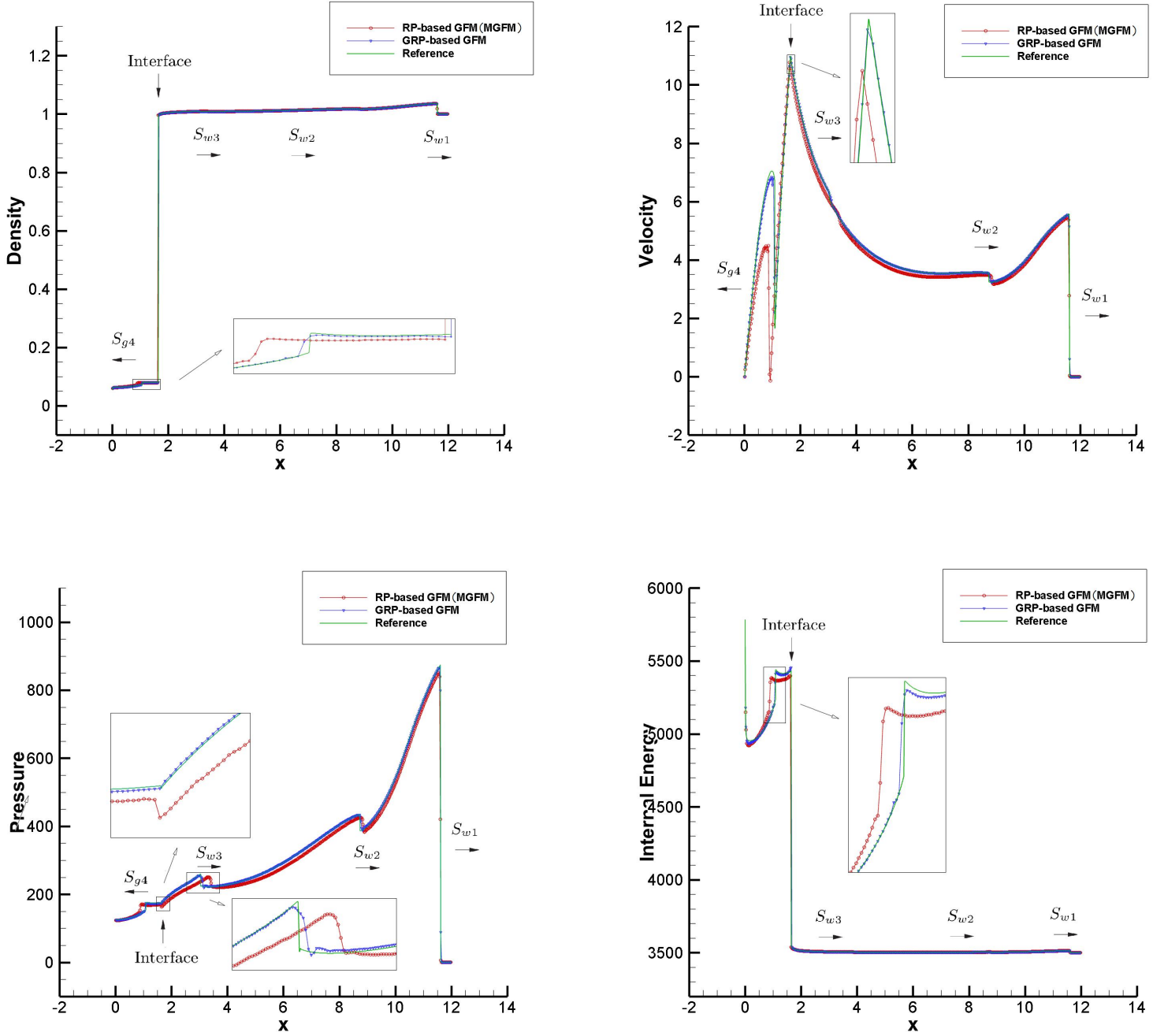

Figure 3.7 Underwater cylindrical symmetrical explositon $(m = 2)$.
The fineness of the mesh is 1/500, the computation time is $t = 0.068$.

4. Two-dimensional compressible multi-medium problem

➢ Mathematical model

$$\frac{\partial U}{\partial t}+\frac{\partial F(U)}{\partial x}+\frac{\partial G(U)}{\partial y}=0,\ \text{for}\ (x,y)\in\Omega, t>0,$$

$$U(x,y,0)=\begin{cases}U_1(x,y,0), & \text{if}\ (x,y)\in\Omega_1^{r,0},\\ U_2(x,y,0), & \text{if}\ (x,y)\in\Omega_2^{r,0},\end{cases}\quad e=\begin{cases}e_1(\rho,p), & \text{if}\ (x,y)\in\Omega_1^{r}(t),\\ e_2(\rho,p), & \text{if}\ (x,y)\in\Omega_2^{r}(t).\end{cases}\tag{4.1}$$

The Interface is $\Gamma(t):\varphi(x,y,t)=0$, where φ is the level - set function.The real fluid region of medium J is denoted as $\Omega_J^r(t)$, and

$\Omega_1^r(t):\varphi(x,y,t)<0,\quad \Omega_2^r(t):\varphi(x,y,t)>0.$

Denote $\Gamma^n=\Gamma(t_n),\ \Omega_1^{r,n}=\Omega_1^r(t_n),\ \Omega_2^{r,n}=\Omega_2^r(t_n).$

The EOS of medium J is $e=e_J(\rho,p),\ J=1,2.$

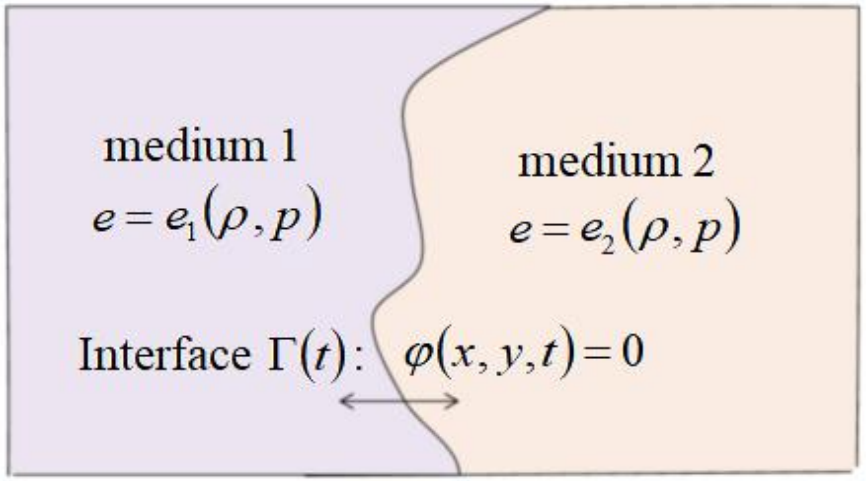

Figure 4.1 The mathematical model for two -dimensional multi-medium problem.

The two-dimensional Euler equations has Galilean invariance, so that the transformed equation will have a source term associated with the tangential direction $-\frac{\partial G(\hat{U})}{\partial \eta}$, when we transform the equations from the coordinate system (x, y) to the coordinte system (ξ, η).

$$\frac{\partial U}{\partial t}+\frac{\partial F(U)}{\partial x}+\frac{\partial G(U)}{\partial y}=0$$

$$\Updownarrow$$

$$\frac{\partial \hat{U}}{\partial t}+\frac{\partial F(\hat{U})}{\partial \xi}+\frac{\partial G(\hat{U})}{\partial \eta}=0$$

$$\Updownarrow$$

$$\frac{\partial \hat{U}}{\partial t}+\frac{\partial F(\hat{U})}{\partial \xi}=\boxed{-\frac{\partial G(\hat{U})}{\partial \eta}}$$

➢ Riemann problem（RP）-based GFM in 2D

Search the nodes which are less than $1.5h$ away from the interface, and then save them into two sets respectively,

$$Q_{\mathrm{J}}^{n}=\left\{P\in\Omega_{\mathrm{J}}^{r,n}\middle|d\left(P,\Gamma_{n}\right)<1.5h\right\},\quad \mathrm{J}=1,2,$$

where $h=\min\left(\Delta x,\Delta y\right)$.

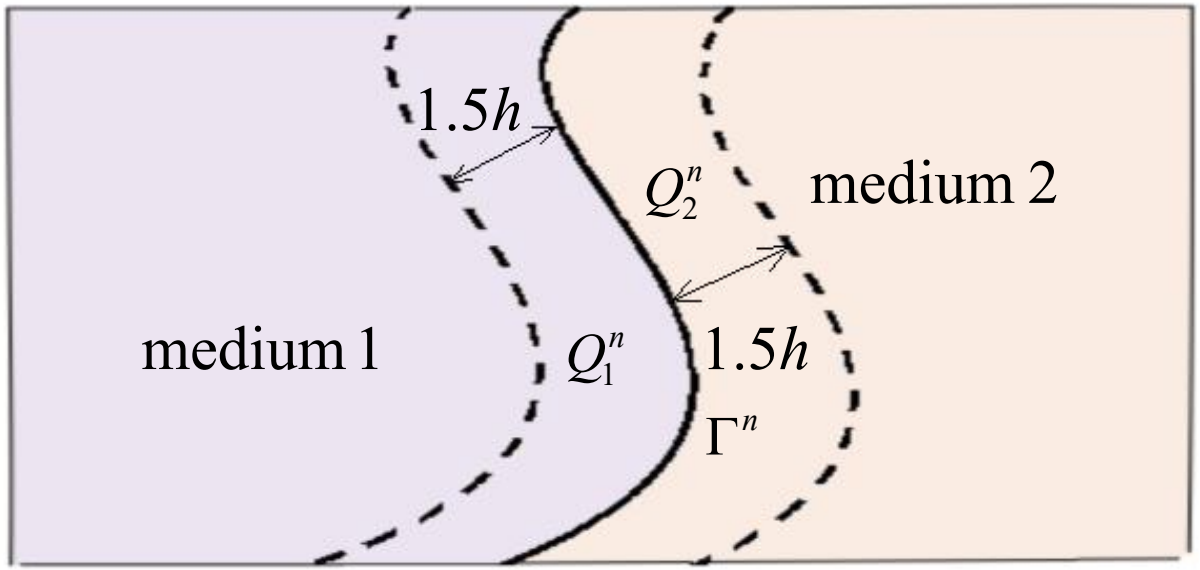

Figure 4.2 Search for the nodes near interfaces in real fluid regions.

Establish a local double - medium RP along the normal direction of the interface Γ^n for $\forall\ P \in Q_{\mathrm{J}}^n$:

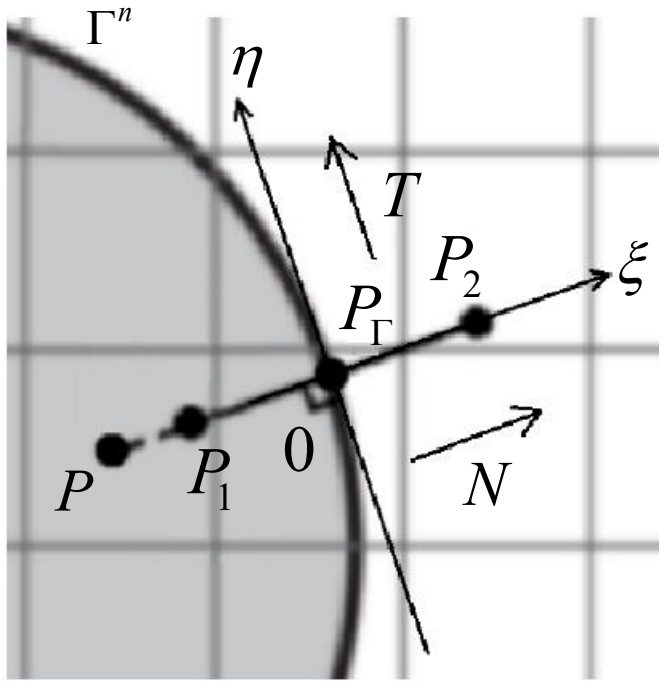

Figure 4.3 Establish a local coodinate system along the tangential and normal directions.

Assuming the vertical point P_Γ as the origin, the normal direction $N = (n_x, n_y)$ as the $\xi-$axis, the tangential direction $T = (t_x, t_y)$ as the $\eta-$axis, Establish a local coordinate system.

Choose two points on both sides of the vertical point P_Γ, satisfying that

$$d(P_{\mathrm{J}}, \Gamma^n) = d(P_{\mathrm{J}}, P_\Gamma) = h, \quad \mathrm{J} = 1,2.$$

The fluid states at P_{J} , i.*e.*,

$$W_{\mathrm{J}} = \left(\rho(P_{\mathrm{J}}), u_x(P_{\mathrm{J}}), u_y(P_{\mathrm{J}}), p(P_{\mathrm{J}})\right)^T, \quad \mathrm{J} = 1,2.$$

can be obtained by bilinear interpolation from the fluid states at the nodes surounding P_{J}.

Establish a local double - medium RP along the normal direction of the interface Γ^n for $\forall P \in Q_{\mathrm{J}}^n$:

The source term is zero

$$\frac{\partial U_\xi}{\partial t}+\frac{\partial F\left(U_\xi\right)}{\partial \xi}=\boxed{0,}\ \text{for } t>t_n, \xi \in(-\delta, \delta),$$

$$U_\xi\left(\xi, t_n\right)=\begin{cases} U_{\xi,1}, & \text{if } \xi<0, \\ U_{\xi,2}, & \text{if } \xi>0, \end{cases} \quad e=\begin{cases} e_1(\rho, p), & \text{if } (\xi, \eta) \in \Omega_1^r(t), \\ e_2(\rho, p), & \text{if } (\xi, \eta) \in \Omega_2^r(t). \end{cases} \tag{4.2}$$

where the vector of primitive variables associated with the vector of conserved variables $U_{\xi,\mathrm{J}}(\xi, \eta)$ is

$$\boxed{W_{\xi,\mathrm{J}}=\left(\rho\left(P_{\mathrm{J}}\right), u_x\left(P_{\mathrm{J}}\right) n_x+u_y\left(P_{\mathrm{J}}\right) n_y, p\left(P_{\mathrm{J}}\right)\right), \quad \mathrm{J}=1,2.}$$

The initial data are constantly distributed

The intermediate states are also constantly distributed

As shown in Figure 4.4, solve the intermediate states of the local double-medium RP (4.2),

$$W_{\xi,\mathrm{J}*}=\left(\rho_{\mathrm{J}*},u_{\xi*},p_*\right)^T,\quad \mathrm{J}=1,2. \tag{4.3}$$

Since $P\in Q_{\mathrm{J}}^n$, modify the fluid states at P by making use of the intermediat states (4.3) associated with medium J,

$$W(P):=\left(\rho_{\mathrm{J}*},u_{\xi*}n_x+u_\eta(P)t_x,u_{\xi*}n_y+u_\eta(P)t_y,p_*\right)^T, \tag{4.4}$$

where $u_\eta(P)=u_x(P)t_x+u_y(P)t_y$ is the original tangential velocity of P.

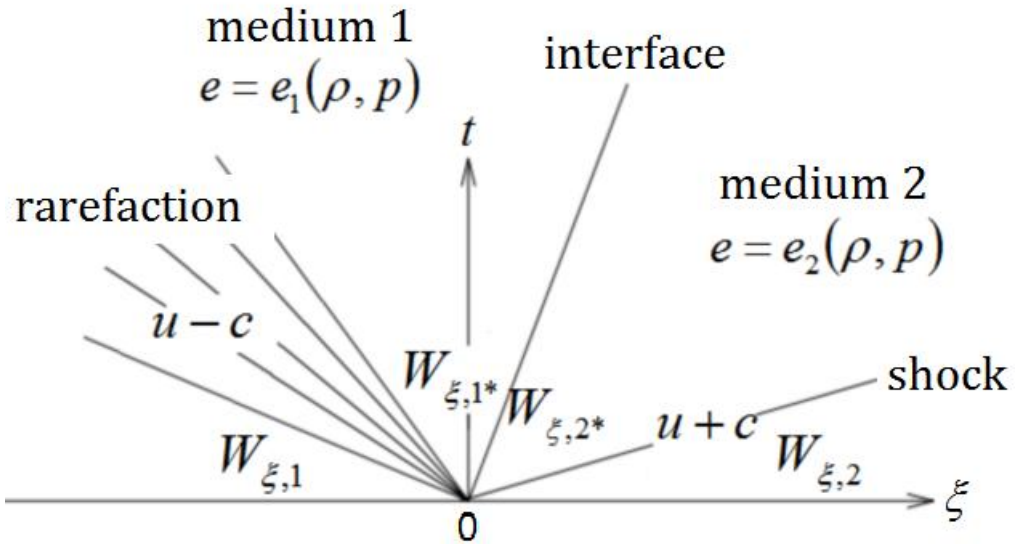

Figure 4.4 The wave structure of local double-medium RP (4.1) .

Extending the modified fluid states in the real fluid regions near the interface to the ghost fluid regions (i.e., $\forall P\in Q_{\mathrm{J}}^n,\ \mathrm{J}=1,2$) by solving the Eikonal equation

$$I_t\pm n\cdot\nabla I=0$$

iteratively.

✓ The disadvantages of the RP-based GFM in 2D

- The effects of the source term associated with the tangential direction can not be reflected.

- There will be mismatch errors near the interface, since the continuity of the material derivatives along the normal direction of pressure and normal velocity can not be maintained.

- The numerical results are not very well, if we obtain the initial data by bilinear interpolation.

- The numerical efficient is very low, if we extend the ghost fluid states by solving the Eikonal equation iteratively, since it needs to traverse the nodes in the ghost fluid regions for 20 to 30 times per time step.

➢ The generalized Riemann problem（GRP）-based GFM

The source term associated with the tangential direction

Establish a local double-medium GRP along the normal direction of the interface for $\forall P \in Q_{\mathrm{J}}^{n}$:

$$\frac{\partial U}{\partial t}+\frac{\partial F(U)}{\partial \xi}=\boxed{-\frac{\partial G(U)}{\partial \eta}},\quad \text{for } t>t_n,(\xi,\eta)\in(-\delta,\delta)\times(-\delta,\delta),$$

$$U(\xi,\eta,t_n)=\begin{cases}U_1(\xi,\eta), & \text{if } \xi<0,\eta\in(-\delta,\delta),\\ U_2(\xi,\eta), & \text{if } \xi>0,\eta\in(-\delta,\delta),\end{cases}\qquad e=\begin{cases}e_1(\rho,p), & \text{if } (\xi,\eta)\in\Omega_1^r(t),\\ e_2(\rho,p), & \text{if } (\xi,\eta)\in\Omega_2^r(t).\end{cases}\tag{4.5}$$

where the vector of primitive variables associated with the vector of conserved variables $U(\xi,\eta)$ is

$$\boxed{W_{\mathrm{J}}(\xi,\eta)=W(P_{\mathrm{J}};\xi,\eta)+\xi\left(\frac{\partial W}{\partial \xi}\right)(P_{\mathrm{J}};\xi,\eta)+\eta\left(\frac{\partial W}{\partial \eta}\right)(P_{\mathrm{J}};\xi,\eta),\quad \mathrm{J}=1,2.}$$

The primitive variables in the intial data are linearly distributed

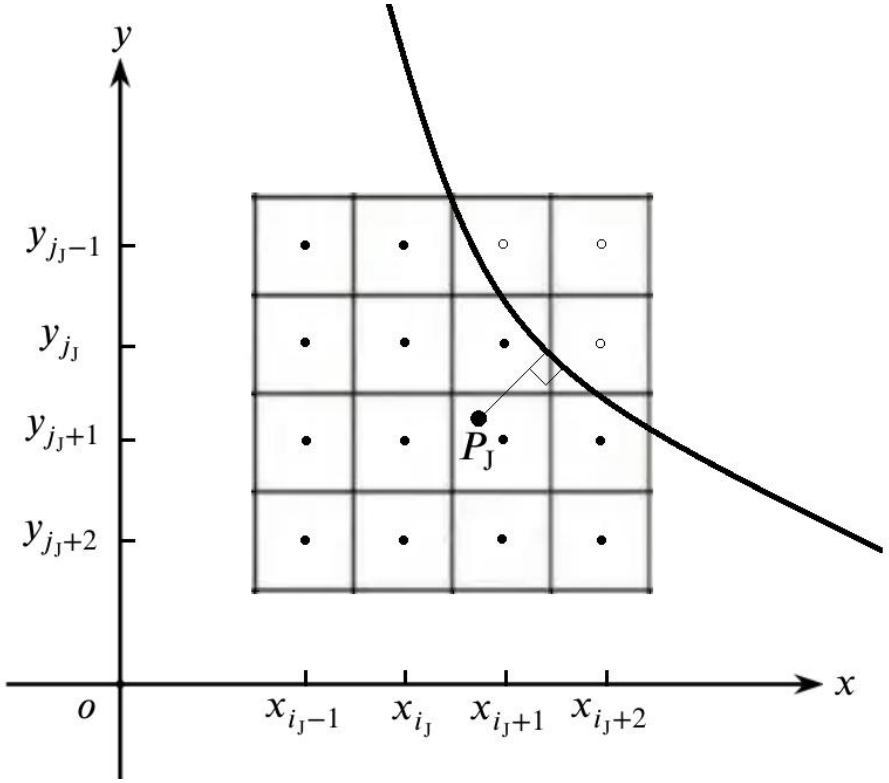

Figure 4.5 Data template for distance weighted least squares fitting.

As shown in Figure 4.5, make use of the nodes in the real fluid region of medium J which are two circles around P_J, to obtain the fluid states at P_J by distance weighted least squares fitting, linearly distributed

$$W(P_J;x,y)+(x-\bar{x}_J)\frac{\partial W}{\partial x}(P_J;x,y)+(x-\bar{y}_J)\frac{\partial W}{\partial y}(P_J;x,y),$$

where $(\bar{x}_J,\bar{y}_J)$ is the coordinate of P_J, $J=1,2.$

As shown in Figure 4.6, firstly, choose the following (4.5) 4.6
as the initial data of the associated RP of the local double-medium GRP (4.4), 4.5

$$U_{\xi}(\xi,t_n)=\begin{cases}U_{1,\xi}, & \text{if } \xi<0,\\ U_{2,\xi}, & \text{if } \xi>0,\end{cases} \tag{4.6}$$

where the vector of primitive variables associated with the vector of conserved variables $U_{\mathrm{J},\xi}$ is $W_{\xi}(P_{\mathrm{J}};\xi,\eta)$, $\mathrm{J}=1,2$,

to obtain the intermediate states $W_{\xi,\mathrm{J}*}=(\rho_{\mathrm{J}*},u_{\xi*},p_*)^T$, $\mathrm{J}=1,2$,

$$W_{\xi,\mathrm{J}*}=(\rho_{\mathrm{J}*},u_{\xi*},u_{\eta}(P_{\mathrm{J}}),p_*)^T,\ \mathrm{J}=1,2.$$

Then choose $\left(\frac{\partial W}{\partial \xi}\right)(P_{\mathrm{J}};\xi,\eta)$, $\left(\frac{\partial W}{\partial \eta}\right)(P_{\mathrm{J}};\xi,\eta)$, $\mathrm{J}=1,2$, as the 4.5
initial data of the local double-medium GRP (4.4), to obtain the spatial derivatives along the normal direction of the interface

$$\left(\frac{\partial W}{\partial \xi}\right)_{\mathrm{J}*}=\left(\left(\frac{\partial \rho}{\partial \xi}\right)_{\mathrm{J}*},\left(\frac{\partial u_{\xi}}{\partial \xi}\right)_{\mathrm{J}*},\left(\frac{\partial u_{\eta}}{\partial \xi}\right)_{\mathrm{J}*},\left(\frac{\partial p}{\partial \xi}\right)_{\mathrm{J}*}\right)^T,\ \mathrm{J}=1,2. \tag{4.7}$$

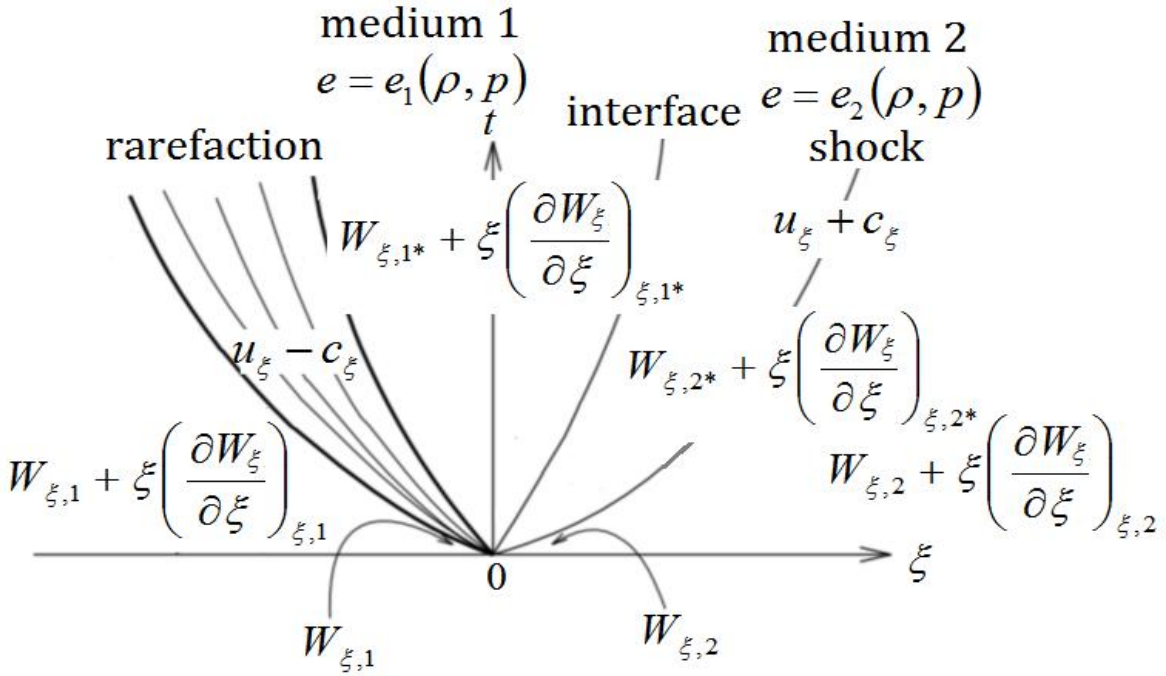

Figure 4.6 The wave structure of local double-medium GRP (4.5) .

The intermediate states are also linearly distributed in computation

First, modify the fluid states at P by making use of the intermediate states of the associated RP of the local double-medium GRP (4.5) as (4.4).

Then modify the spatial derivatives along the normal direction of the fluid states at P by the slopes of the intermediate states of the local double-medium GRP (4.5).

$$\frac{\partial W}{\partial x}(P;x,y) := \left(\frac{\partial W}{\partial \xi}\right)_{\mathrm{J}^*}(x,y)n_x + \frac{\partial W}{\partial \eta}(P;x,y)t_x,$$

$$\frac{\partial W}{\partial y}(P;x,y) := \left(\frac{\partial W}{\partial \xi}\right)_{\mathrm{J}^*}(x,y)n_y + \frac{\partial W}{\partial \eta}(P;x,y)t_y,$$

where $W(x,y) = (\rho, u_\xi n_x + u_\eta t_x, u_\xi n_y + u_\eta t_y, p)$.

Extend the fluid states and the spatial derivatives of them at $\forall P \in Q_{\mathrm{J}}^{n}$ to the ghost fluid region of medium J by linear and constant extrapolation, $\mathrm{J} = 1,2$.

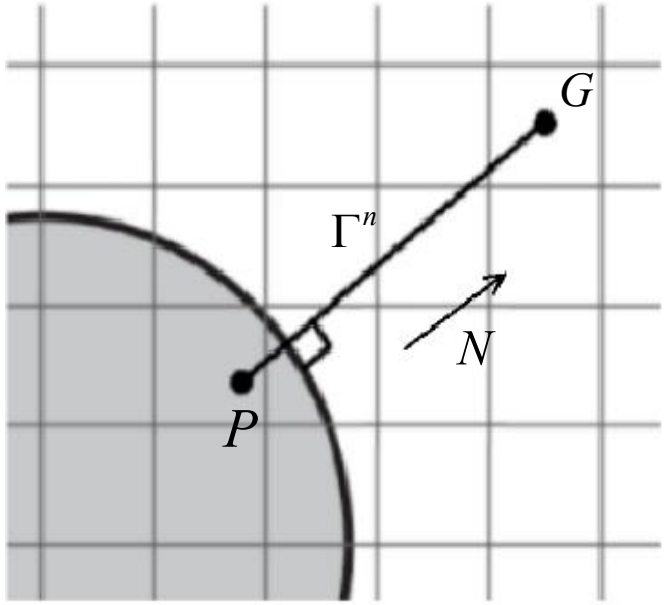

Figure 4.7 Extension by linear and constant extrapolation.

$$N \approx \frac{\nabla \varphi}{|\nabla \varphi|}(G), \quad d\left(G, \Gamma^{n}\right) \approx \varphi(G), \quad |GP| = \operatorname{sign}\left(d\left(G, \Gamma^{n}\right)\right)0.75h + d\left(G, \Gamma^{n}\right).$$

$$\rho(G) = \rho(P) + |GP| \nabla \rho(P) \cdot N, \quad p(G) = p(P) + |GP| \nabla p(P) \cdot N,$$
$$u_{\xi}(G) = u_{\xi}(P) + |GP| \nabla u_{\xi}(P) \cdot N, \quad u_{\eta}(G) = u_{\eta}(P) + |GP| \nabla u_{\eta}(P) \cdot N,$$
$$u_{x}(G) = u_{\xi}(G) n_{x} + u_{\eta}(G) t_{x}, \quad u_{y}(G) = u_{\xi}(G) n_{y} + u_{\eta}(G) t_{y}.$$

$$\frac{\partial W}{\partial x}(G) = \frac{\partial W}{\partial x}(P), \quad \frac{\partial W}{\partial y}(G) = \frac{\partial W}{\partial y}(P).$$

The spatial derivatives of the intermediate states （4.7）of the double-medium GRP（4.5）:

Firstly, consider the effects along the normal direction, secondly, consider the effects along the tangential direction, finally, combined with two-dimensional Euler equations, by making use of the derivatives of each primitive variables with respect to time and tangential directions, we can obtain the derivatives of each primitive variables with respect to normal direction.

Along the normal direction, establish an equation for the material derivatives along the normal direction of normal velocity and pressure. According to the continuity of them across the interface respectively, i.e.,

$$\left(\frac{\widetilde{D}u_\xi}{\widetilde{D}t}\right)_{1*}=\left(\frac{\widetilde{D}u_\xi}{\widetilde{D}t}\right)_{2*}\overset{\Delta}{=}\left(\frac{\widetilde{D}u_\xi}{\widetilde{D}t}\right)_{*},\quad \left(\frac{\widetilde{D}p}{\widetilde{D}t}\right)_{1*}=\left(\frac{\widetilde{D}p}{\widetilde{D}t}\right)_{2*}\overset{\Delta}{=}\left(\frac{\widetilde{D}p}{\widetilde{D}t}\right)_{*},$$

where $\frac{\widetilde{D}}{\widetilde{D}t}=\frac{\widetilde{\partial}}{\widetilde{\partial}t}+u_\xi\frac{\widetilde{\partial}}{\widetilde{\partial}\xi}$ is the material derivatives along the normal direction, combining the two equations, we have

$$\begin{cases} a_1\left(\frac{\widetilde{D}u_\xi}{\widetilde{D}t}\right)_{*}+b_1\left(\frac{\widetilde{D}p}{\widetilde{D}t}\right)_{*}=d_1, \\ a_2\left(\frac{\widetilde{D}u_\xi}{\widetilde{D}t}\right)_{*}+b_2\left(\frac{\widetilde{D}p}{\widetilde{D}t}\right)_{*}=d_2. \end{cases}$$

Along the tangential direction, we obtain the effects along the tangential direction by comparing the difference of the one-dimensional and two-dimensional Euler equations.

✓ The advatages of the GRP-based GFM in 2D

- Reflect the effects of the source term associated with the tangential direction.

Since the two-dimensional Euler equations have Galilean invariance under orthogonal coordinate transformation, there will be a source term associated with the tangential terms in the transformed equations in the local double-medium problem at the interface. However, the effects of this source term can not be reflected by the intermediate states of RP, but can be reflected by the intermediate states of GRP, as the spatial derivatives of the latter are not zero, but the spatial derivatives of the former are zero.

- Eliminate the mismatch errors near the interface.

The ghost fluid states defined by the GRP-based GFM can maintain the continuity of the material derivatives along the normal direction of the normal velocity and pressure across the interface,

$$\frac{\tilde{D}u_{\xi}}{\tilde{D}t}\left(P_{\Gamma^n}-0\right)=\frac{\tilde{D}u_{\xi}}{\tilde{D}t}\left(P_{\Gamma^n}+0\right),\quad \frac{\tilde{D}p}{\tilde{D}t}\left(P_{\Gamma^n}-0\right)=\frac{\tilde{D}p}{\tilde{D}t}\left(P_{\Gamma^n}+0\right).$$

- Improve the method of choosing the initial data of the local double-medium problem.

We obtain the linear distributed initial data by distance weighted least square fitting, and make use of the fluid states at the nodes which are located in the real fluid region and two circles around the point to chose the initial data. Compared with chosing the initial data by bilinear interpolation, the numerical simulation effects are improved substantially.

- Improve the numerical efficiency of extending the ghost fluid states.

We extend the ghost fluid states by linear and constant extrapolation. Compared with extending the ghost fluid states by solving the Eikonal equation iteratively, the numerical efficiency of extending the ghost fluid states are increased, since the former needs to traverse the nodes in the ghost fluid regions for 20 to 30 times per time step, while the latter only needs to traverse the nodes in the ghost fluid regions once per time step.

✓ Numerical results in 2D

In the numerical tests in 2D, we will compare the numerical results of the four methods in Chart 4.2. The EOS of the mediums in this section can be written in (4.8) uniformly,

$$e = \frac{p + \gamma p_\infty}{(1 \quad \gamma)\rho}, \qquad (4.8)$$

For each medium, the coefficients in EOS (4.8) are listed in Chart 4.1.

medium	γ	p_∞
water	7.0	3309
gas	1.4	0
helium	1.648	0
SF6	1.093	0

Chart 4.1 The coefficients in the stiffen gas EOS (4.6).

	The choice for the initial data of the double-medium problem	Types of RP	The way to extend the ghost fluid states	The velocity used to update the level-set function
Method (I)	Bilinear interpolation	RP	Solving the Eikonal equation iteratively	Initial time velocity
Method (II)	Weighted least square fitting to obtain linear distributed initial data, just take the constant part	RP	Solving the Eikonal equation iteratively	Initial time velocity
Method (III)	Weighted least square fitting to obtain linear distributed initial data	GRP	Extend the ghost fluid states and the spatial derivatives of them by linear and constant extrapolation	Initial time velocity
Method (IV)	Weighted least square fitting to obtain linear distributed initial data	GRP	Extend the ghost fluid states and the spatial derivatives of them by linear and constant extrapolation	Middle time velocity

Chart 4.2 Four methods.

Example 1（The shock induced collapse of a helium bubble in air）

As shown in Figure 4.12, the left and right sides are nonreflective boundary condition, and the upper and lower sides are reflective boundary condition, the computation domain is $[0,0.65]\times[\ 0.089,0.089]$, and the number of the mesh is 420×115.

The initial states for helium are

$$(\rho_1,u_{x1},u_{y1},p_1)=(0.182,0,0,10^5).$$

The initial states for air are

$$(\rho_1,u_{x2},u_{y2},p_2)=\begin{cases}(1,0,0,10^5), & x\le 0.32+r,(x-0.32)^2+y^2>r^2(\text{pre-shock}),\\ (1.37636,-124.824,0,156980), & x>0.32+r,(x-0.32)^2+y^2>r^2(\text{post-shock}).\end{cases}$$

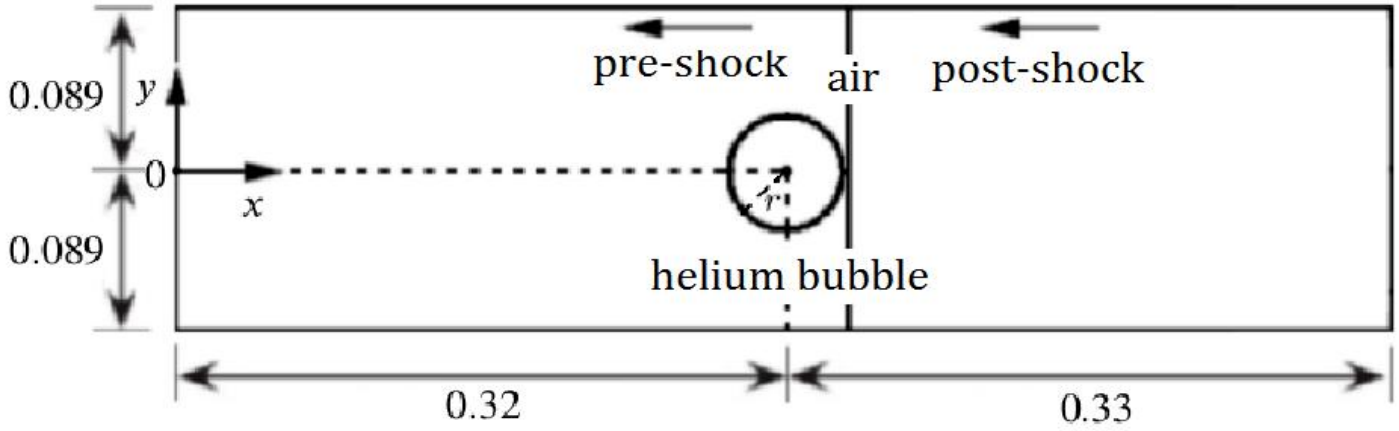

Figure 4.8 Schematic of initial flow configuration for "the shock induced collapse of a helium bubble in air".

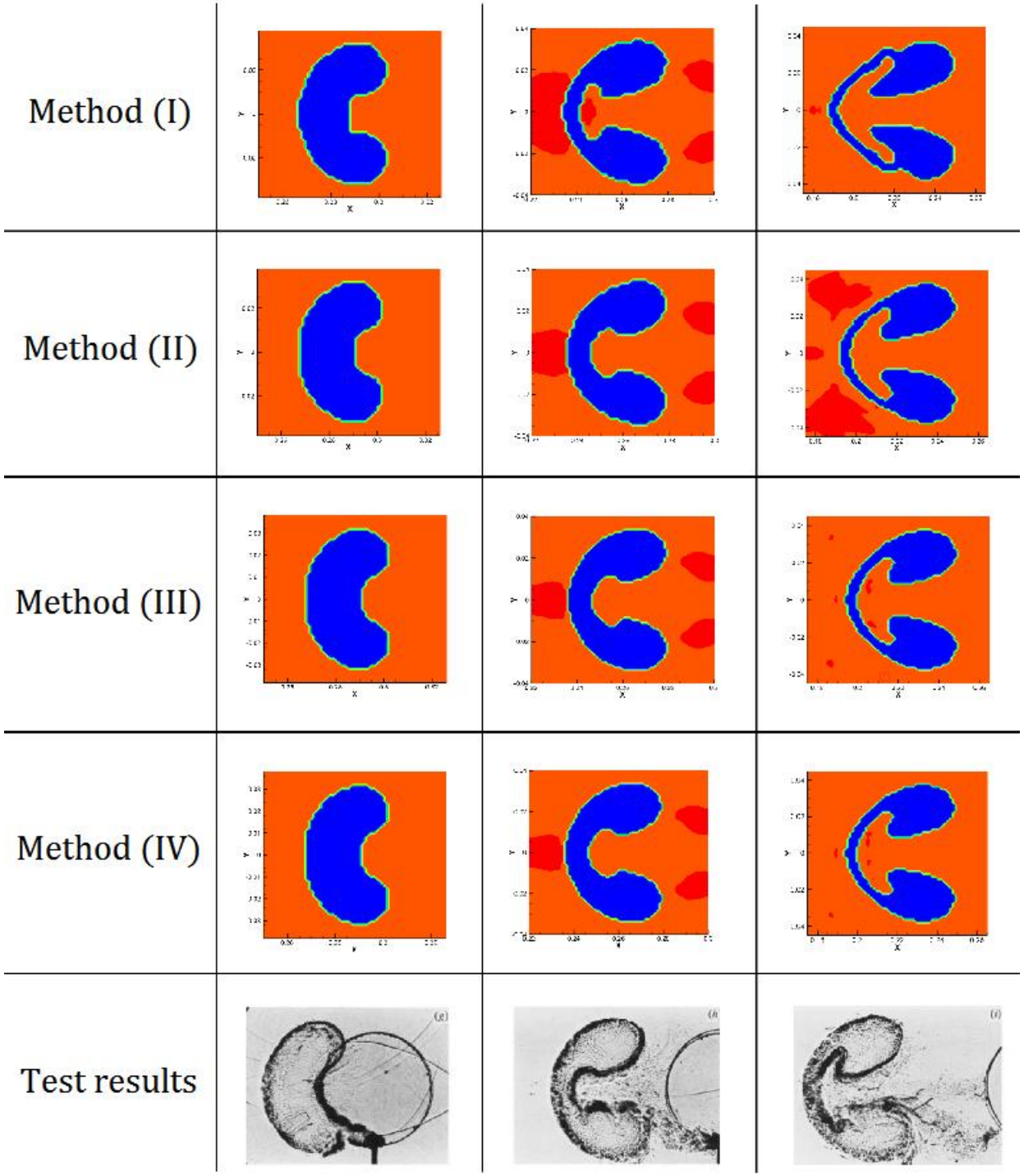

Figure 4.9 Comparison of the simulation results against the experiment results of Hass and Sturtevant (Fig.7 of page 52) for "The shock induced collapse of a helium bubble in air".

Example 2（Richtmyer-Meshkov instability）

As shown in Figure 4.15, the left and right sides are nonreflective boudary condition, and the upper and lower sides are reflective boundary condition, the computation domain is $[4,1]$, the number of the mesh is 400×100.

The initial states for SF6 are

$$(\rho_1, u_{x1}, u_{y1}, p_1) = (5.04,0,0,1.0), \quad 0 \le x \le x_\Gamma(y),\ y \in [0,1],$$

where $x_\Gamma(y) = x_0 - \varepsilon\cos(2\pi k y),\ y \in [0,1]$.

The initial states for air are

$$(\rho_2, u_{x2}, u_{y2}, p_2) = \begin{cases} (1.0,0,0,1.0), & x_\Gamma < x \le 3.0,\ y \in [0,1]\ (\text{pre-shock}), \\ (1.628,0.39,0,1.411), & 3.0 < x \le 4.0,\ y \in [0,1]\ (\text{post-shock}). \end{cases}$$

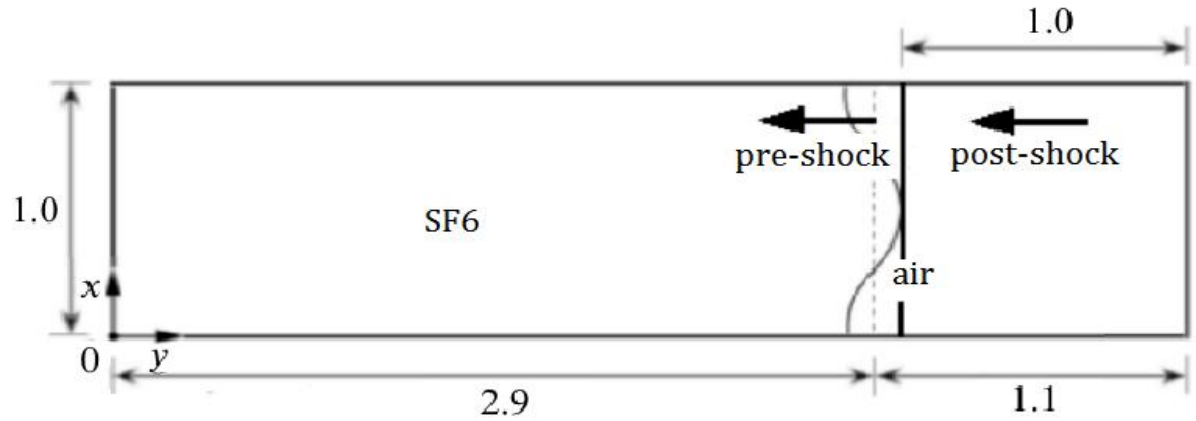

Figure 4.10 Schematic of initial flow configuration "Richtmyer – Meshkov instabiliy".

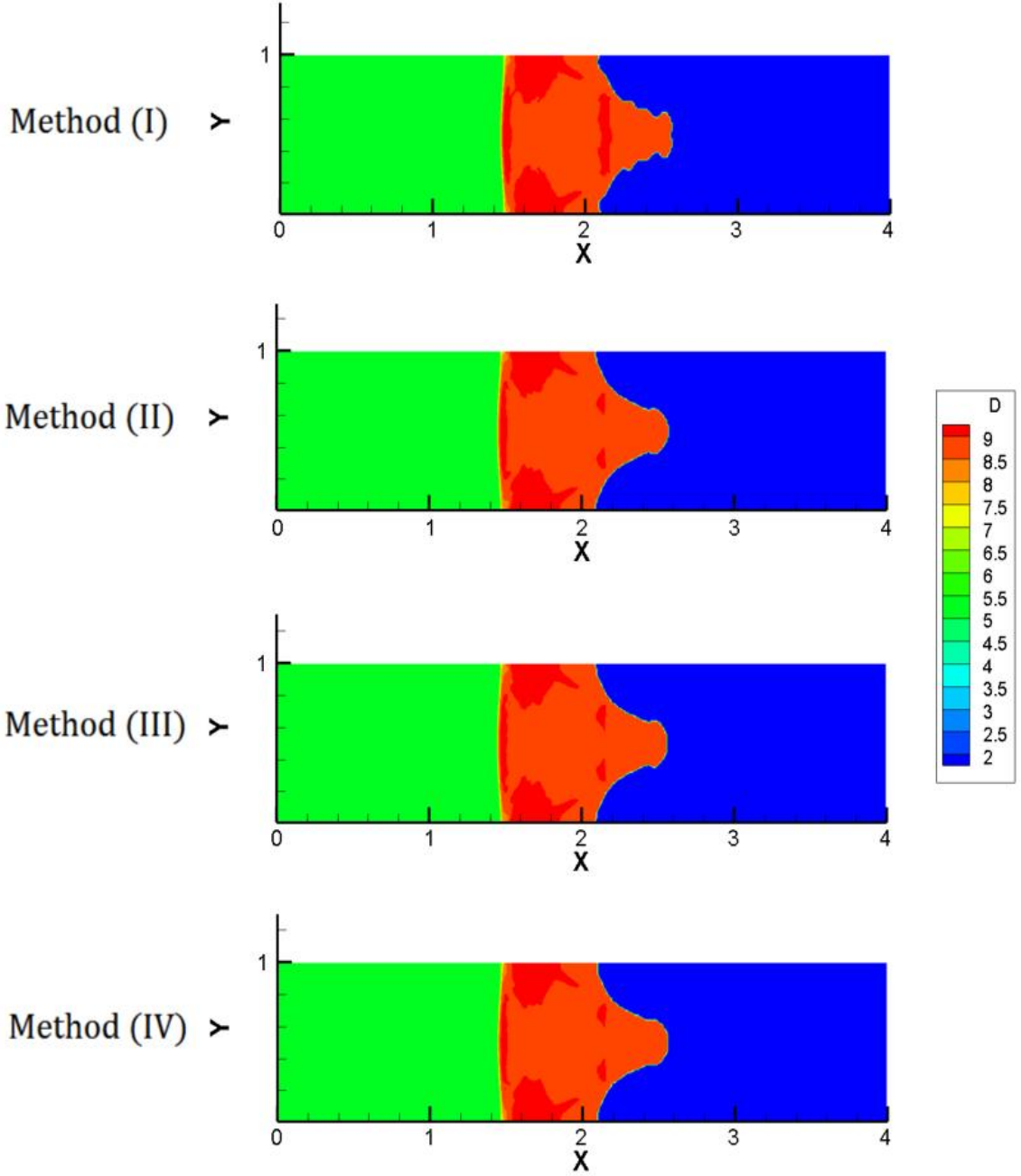

Figure 4.11 Contour maps for density at $t = 2.31$ for "Richtmyer – Meshkov instability".

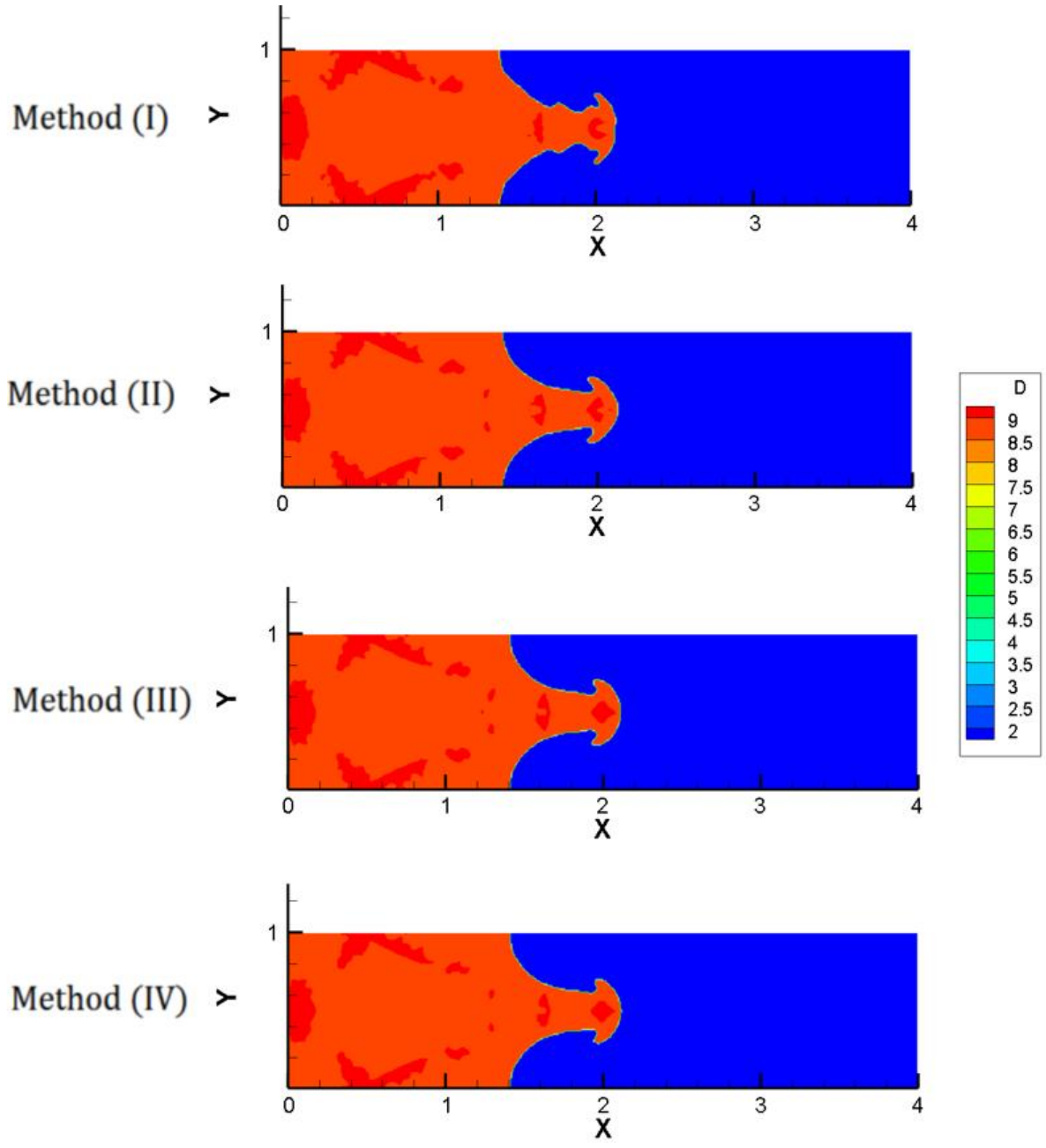

Figure 4.12 Contour maps for density at $t = 4.62$ for "Richtmyer – Meshkov instability".

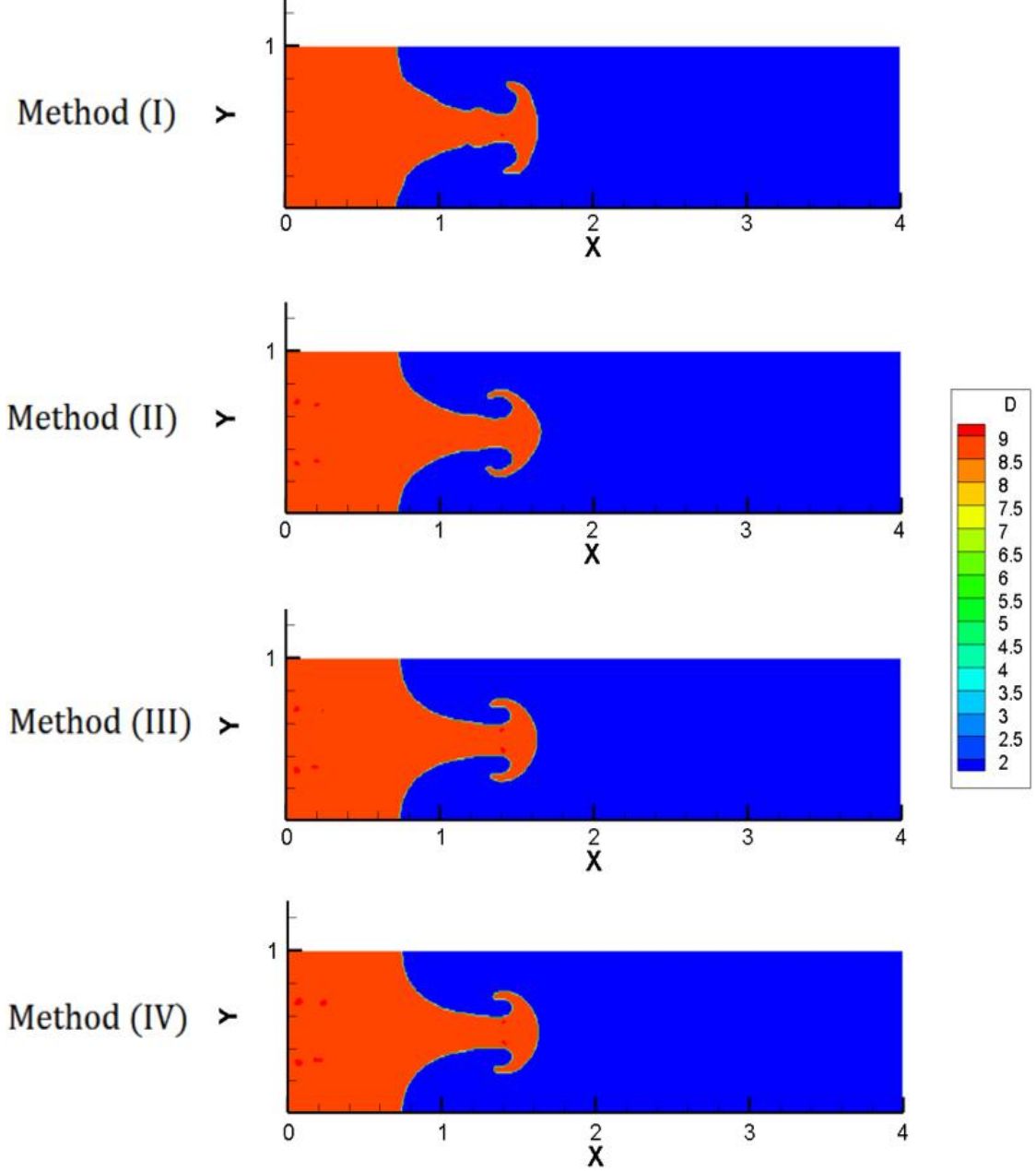

Figure 4.13 Contour maps for density at $t = 6.93$ for "Richtmyer – Meshkov instability".

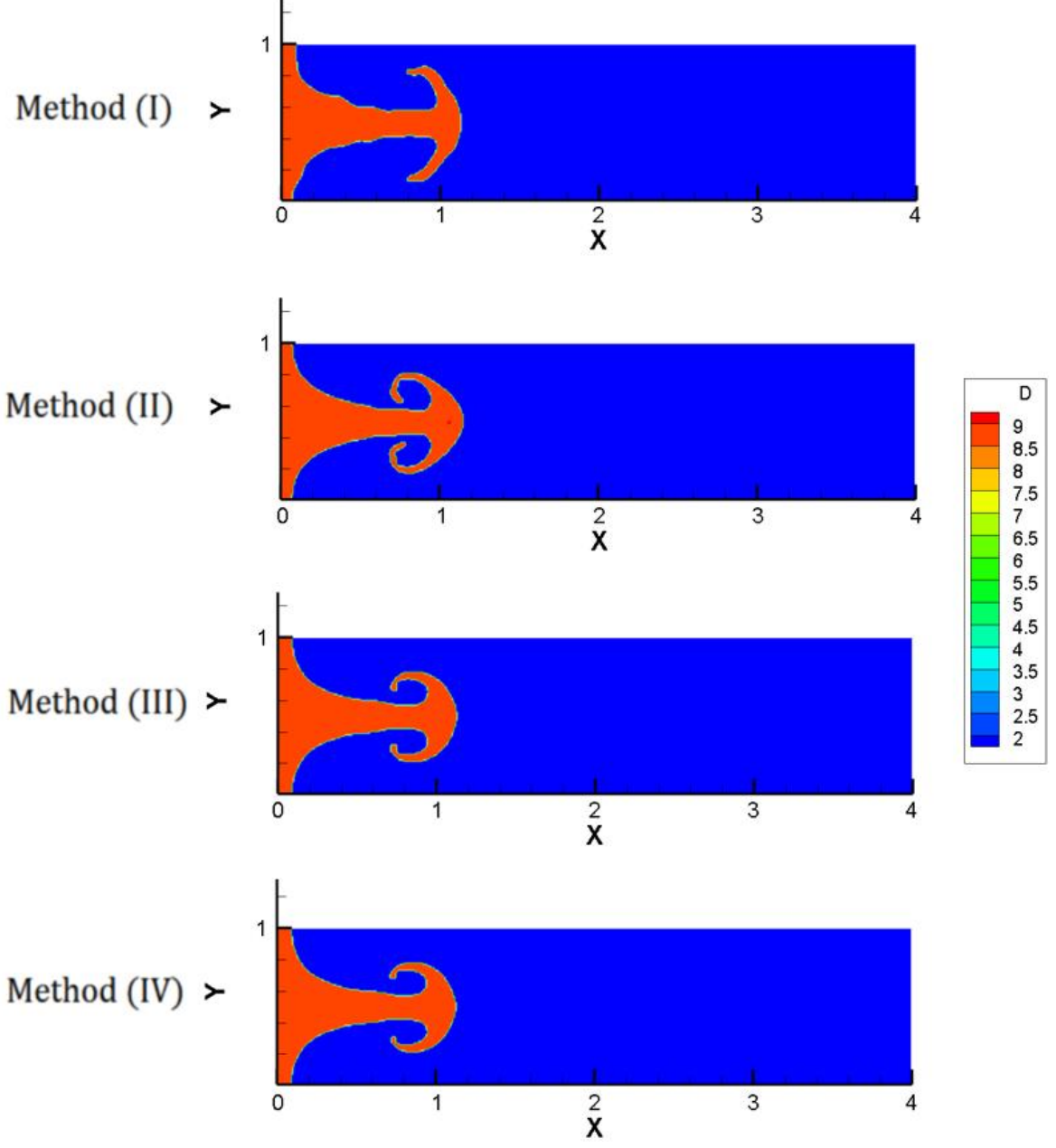

Figure 4.14 Contour maps for density at $t = 9.24$ for "Richtmyer – Meshkov instability".

Method	Time steps	Total extension time	Average extension time
Method (I)	1382	2.86×10^{2}s	2.07×10^{-1}s
Method (II)	1369	3.00×10^{2}s	2.29×10^{-1}s
Method (III)	1363	6.99s	5.13×10^{-3}s
Method (IV)	1363	6.60s	4.84×10^{-3}s

Chart 4.3 Time cost on fluid extension for "The shock induced collapse of a helium bubble in air".

Method	Time steps	Total extension time	Average extension time
Method (I)	3901	1.27×10^{3}s	3.26×10^{-1}s
Method (II)	3910	1.32×10^{3}s	3.37×10^{-1}s
Method (III)	3836	3.58×10^{1}s	9.33×10^{-3}s
Method (IV)	3834	3.31×10^{1}s	8.65×10^{-3}s

Chart 4.4 Time cost on fluid states extension for "Richtmyer Meshkov instability".

Thanks and Questions